Journal of Solid State Chemistry 184 (2011) 1603–1607

Contents lists available at ScienceDirect

Journal of Solid State Chemistry

journal homepage: www.elsevier.com/locate/jssc

SiO_2 nanospheres with tailorable interiors by directly controlling Zn^{2+} and $NH_3 \cdot H_2O$ species in an emulsion process

Yuchao Liao [a,b], Xiaofeng Wu [a], Zhen Wang [a,b], Yun-Fa Chen [a,*]

[a] State Key Laboratory of Multiphase Complex Systems, Institute of Process Engineering, Chinese Academy of Sciences, Beijing 100190, China
[b] Graduate University of Chinese Academy of Sciences, Beijing 100049, China

ARTICLE INFO

Article history:
Received 30 November 2010
Received in revised form
19 March 2011
Accepted 29 March 2011
Available online 30 April 2011

Keywords:
SiO_2 nanospheres
Tailorable interior
Microemulsion
Temporary template
Ostwald Ripening

ABSTRACT

SiO_2 nanospheres with tailorable interiors were synthesized by a facile one-spot microemulsion process using TEOS as silica source, wherein cyclohexane including triton X-100 and *n*-octanol as oil phase and Zn^{2+} or $NH_3 \cdot H_2O$ aqueous solution as dispersive phase, respectively. The products were characterized by Scanning Electron Microscopy, Transmission Electron Microscopy and X-ray Powder Diffraction. It was suggested that the as-synthesized silica nanospheres possessed grape-stone-like porous or single hollow interior, and also found that the ammonia dosage and aging time played key roles in controlling the size and structure of silica nanospheres. Furthermore, the comparative results confirmed that in-situ zinc species [$ZnO/Zn(OH)_2$] acted as the temporary templates to construct grape-stone-like interior, and a simultaneously competing etching process occurred owing to the soluble $Zn(NH_3)_4^{2+}$ complex formation while the additional excessive ammonia was introduced. With the aging time being extended, the in-situ nanocrystals tended to grow into bigger ones by Ostwald Ripening, producing single hollow interior.

1. Introduction

Porous materials have opened many new applications such as catalysis, separation, thermal insulation and nanoscience due to their respective high specific surface areas, tunable pore sizes and high porosity. Hollow interior structure had attracted much more attention in recent years, which was applied extensively in catalysis [1,2], sensors [3], Li-ion batteries [4,5], microreactors [6,7], biomedicines [8,9] and so on. Many methods such as template method [10–13], template-free method [14,15], sacrificial template method [16], Kirkendall effect [17–19], galvanic replacement [20,21], have been introduced to prepare hollow interior structure. Among them, the template method is an effective and intriguing strategy, in which the templates are firstly prepared, then the surface of templates is functionalized and coated with target materials or their precursors, particles with core–shell structure can be obtained. As the core–shell particles roasted in air or etched with an appropriate solvent, the hollow interior structure can be obtained. Generally, various templates such as PS spheres [22], PMMA spheres [23], C spheres [24], and SiO_2 spheres [25], droplets [26], vesicles [27,28] are used. However, preparation procedures of templates usually take much time, and the removal of templates by either sintering or etching is very complicated, time-consuming and energy-consuming. Moreover, the hollow structures obtained via template-mediated approach are usually larger than 100 nm because it is hard to make smaller size template particles, which limits the application of this method. While microemulsion method proposed first by Schulman [29] would overcome the shortcomings above because the size of dispersed droplets is usually less than 100 nm. In addition, the advantages including mild experiment conditions and simple procedures make microemulsion technology a facile and efficient method for synthesizing various nano-sized materials.

In this present work, SiO_2 nanospheres with tailorable interiors were obtained through just controlling the reactants dosage and aging time of temporary templates in microemulsions. The temporary templates were firstly produced by two microemulsions, and then they would be coated with SiO_2 shells derived from TEOS and synchronously etched due to the addition of third microemulsion. As the hydrolysis rate of TEOS is a little faster than etching rate of the temporary templates, nanostructured interior structures were obtained. In contrast to conventional methods, no additional processes such as roasting or etching were needed. And the size of the particles could be tuned within 100 nm. Moreover, the nanostructured single or multiple interior could be achieved by just only controlling the aging time of temporary templates. To the best of our knowledge, this technique in which tailorable interiors were

* Correspondence to: Institute of Process Engineering, Zhongguancun Beiertiao 1#, Haidian District, Beijing, China. Fax: +86 10 62525716.
E-mail address: yfchen@home.ipe.ac.cn (Y.-F. Chen).

0022-4596/$ - see front matter © 2011 Elsevier Inc. All rights reserved.
doi:10.1016/j.jssc.2011.03.051

prepared by directly controlling reactive species has not been reported previously.

2. Experimental

2.1. Materials

Ethanol, ammonia, tetraethoxysilane (TEOS) and $Zn(NO_3)_2$, were of analytic grade and purchased from Beijing Vas Chemical Reagent Co, Ltd., China. Cyclohexane, triton X-100, *n*-octanol were of analytical grade and provided by Beijing Yili Chemical Reagent Co, Ltd., China. Deionized water was used for all processes.

2.2. Synthesis of SiO_2 nanoparticles with tailorable interior

Three cyclohexane emulsified systems including different dispersive phase were prepared before reaction. All the microemulsions mentioned above had fixed amount of oil phase including 10 mL cyclohexane, 1.5 mL triton X-100 and 1 mL *n*-octanol, and were indexed as MA with $Zn(NO_3)_3$ solution as dispersive phase, MB with dilute ammonia and MC with concentrated ammonia. Agitation (1000 rpm) or ultrasound (40 k Hz, 400 W) was applied to make microemulsions transparent/translucent and stable. First, MA and MB of equal volumes were simultaneously poured into a beaker, and the aging time was kept for 0.5–48 h. After the prescribed time, MC and a certain amount of TEOS were sequentially added into the system. Half an hour later, the mixture including MA, MB, MC and TEOS was stopped agitating to age for 24 h. Then the mixture was demulsified, washed and centrifuged with ethanol by three cycles. The final particles were obtained after drying at 80 °C for 12 h, the atmosphere was air.

2.3. Characterizations

X-Ray Powder Diffraction (XRD) data were collected on the X'Pert Pro powder diffractometer. Scanning Electron Microscopy (SEM) of type JSM-6700 F, JEOL, was used to characterize the morphologies of the products. Transmission electron microscopy (TEM) images and Energy Dispersive Spectrometry (EDX) were obtained on a JEM 2010 F operated at 200 kV. Fourier Transfer infrared spectrums (FT-IR) were obtained on Tensor 37 type from Brucker Company. The microemulsion droplets size was determined using dynamic light scattering technology (DLS) on Dyna-Pro Nanostar from Wyatt Technology Corporation.

3. Results and discussion

3.1. Effect of temporary templates on the interior structure of products

Generally, the existence and the shape of the templates are the critical parameters affecting the interior structure of porous materials. Here MA and MB without the addition of MC and TEOS produced zinc species acting as the temporary templates. The composition and crystal type of temporary templates were identified by X-Ray Powder Diffraction (XRD). As shown in Fig. 1(A), the peaks locating near 33°, 58° and 69° can be indexed to ZnO phase (JCPDS Card No 21-1486), and the peaks near 27°, between 31° and 34° can be indexed to $Zn(OH)_2$ phase (JCPDS Card No 20-1435). The component of temporary templates was further confirmed by IR spectrum as shown in Fig. 2(A). The peaks between 400 and 600 cm^{-1} are attributed to the stretching vibrations of Zn–O, and the peak at 3459 cm^{-1} to the stretching vibration of O–H. As for the hydroxyl coordination compound, the flexural vibration peak of M–OH tends

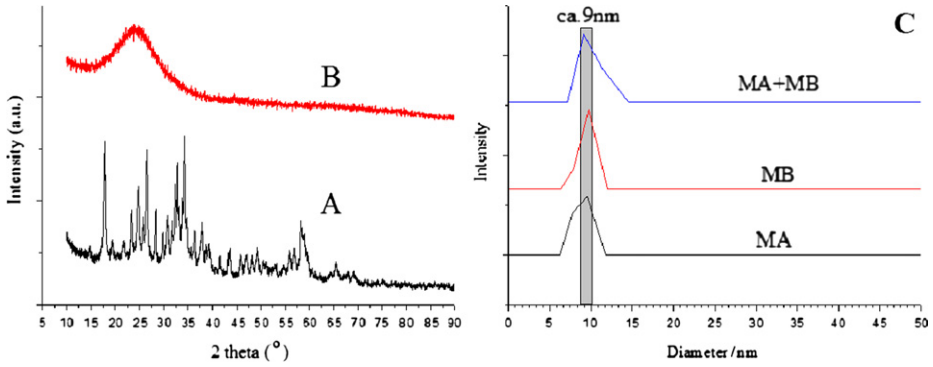

Fig. 1. XRD patterns of temporary templates (A) and SiO_2 nanospheres (B) and dynamic light scattering spectra of MA, MB and mixture of them (C).

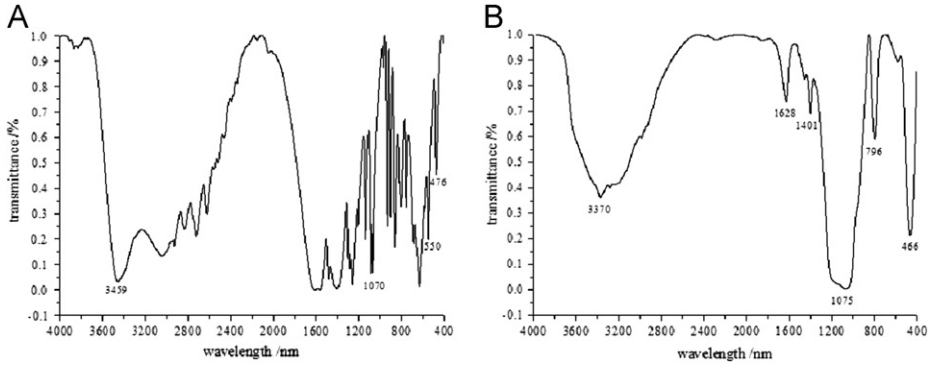

Fig. 2. FT-IR spectra of temporary templates (A) and SiO_2 nanospheres (B).

to appear below 1200 cm^{-1} [30], so the peak at 1070 cm^{-1} is attributed to the flexural vibration Zn–OH. The analysis above indicates the temporary templates of a mixed crystal of ZnO and $Zn(OH)_2$. The size of the temporary templates is certain to affect that of interior structure of final products. Hence, the droplets size of MA, MB and mixture of them was investigated using dynamic light scattering (DSL) technology. The results in Fig. 1(C) show that the size (ca. 9 nm in diameter) of MA or MB scarcely changes before mixing and after mixing. To avoid the changes in droplets size, in all experiments MA and MB have identical oil phase and the equal volumes of water phase. When MC was added, the translucent mixture of MA and MB became transparent and no products were collected. It may be attributed to the transformation of zinc species into soluble complex $Zn(NH_3)_4^{2+}$. MC and TEOS were used and produced dense nanospheres with ca. 35 nm in diameter in the absence of MA and MB as shown in Fig. 4(A). The possible reason is explained as following: after the addition of MC, the TEOS molecules diffuse onto the interface between oil phase and aqueous droplets and start to react with H_2O under alkaline condition. The details of hydrolysis and condensation of TEOS were interpreted in previous studies [31,32]. Because of no templates in the aqueous phase, hydrolysis products of TEOS become more and more hydrophilic and dissolve in the aqueous droplets. Afterwards, nanocrystals precipitate from the supersaturated solution, aggregate and grow into dense spheres. From the facts mentioned above, it is ascertained that the in-situ generated zinc species nanocrystals act as temporary templates to shape the interior structure of particles.

Table 1
Experimental conditions.

Sample	C_A[a],V_A[b]	C_B[c]V_B[d]	V_C[e]	AT[f]	TEOS[g]	Display
1	–	–	0.5	–	0.5	Fig. 4(A)
2	0.2, 1	0.4, 1	0.5	0.5	0.5	Fig. 4(B)
3	0.2, 1	0.2, 1	0.5	0.5	0.5	Fig. 4(C)
4	0.2, 1	0.6, 1	0.5	0.5	0.5	Fig. 4(D)
5	0.4, 2	0.8, 2	0.5	0.5	0.5	Fig. 4(E)
6	0.2, 1	0.4, 1	0.5	12	0.5	Fig. 4(F)
7	0.2, 1	0.4, 1	0.5	24	0.5	Fig. 4(G)
8	0.2, 1	0.4, 1	0.5	48	0.5	Fig. 4(H)

[a] Concentration of Zn^{2+} solution in MA (mol/L).
[b] Volume of Zn^{2+} solution in MA (mL).
[c] Concentration of dilute ammonia solution in MB (mol/L).
[d] Volume of dilute ammonia solution in MB (mL).
[e] Volume of concentrated ammonia solution in MC (mL).
[f] The aging time of zinc species produced by MA and MB (h).
[g] The volume of TEOS (mL). The composition of oil phase in all microemulsion is identical.

3.2. Identification of hollow-interior-nature of products

According to Table 1, Sample 2 was firstly produced. SEM image (Fig. 4(B) inset) shows the particles of uniform size with well dispersion. The corresponding TEM image (Fig. 4(B)) shows an obvious contrast between the dark edge and the pale interior of the individual spheres, indicative of porous grape-stone-like interiors with ca. 10 nm in diameter and shell with ca. 15 nm in thickness. Excitingly the interior size is very close to that of the temporary templates mentioned earlier. In the corresponding FT-IR spectrum of Fig. 2(B), the adsorption peak at 1075 cm^{-1} is attributed to the antisymmetric stretching vibration of Si–O–Si, and the two peaks at 796 cm^{-1} and 466 cm^{-1} correspond to the flexural vibration of Si–O–Si. The HRTEM technique (Fig. 3(A)) indicates the particle shell of amorphous type without crystal lattices, and there are two obvious strong peaks for Si and O in the EDX spectrum (Fig. 3(B)). Here it should be noted that the weak peaks for C and Cu are derived from carbon membrane and copper mesh of sample holder. It is ascertained that the component of particle shell is amorphous SiO_2. Furthermore it is found from XRD patterns in Fig. 1(B) that a single broad peak at $2\theta=23^\circ$ attributed to the silica amorphous phase, and no obvious characteristic responses of zinc species are identified. All the analysis above indicates that zinc species are dissolved in the etching process and SiO_2 nanospheres with hollow-interior are formed.

3.3. Effects of dilute ammonia concentration and aging time of temporary templates on the interior structure of products

In order to investigate the possible formation process and mechanism of the nanostructured silica nanospheres, the parameters including reactant dosage and aging time were further studied. It is to be remarked that the amount of MC and TEOS were fixed in all of the experimental conditions. First, the influence of $NH_3 \cdot H_2O$ concentration in MB on interior structure of nanospheres was investigated under the condition that Zn^{2+} concentration (0.2 mol/L) in MA was fixed. As 0.2 mol/L $NH_3 \cdot H_2O$ in MB was used and dense particles with ca. 30 nm in diameter formed as shown in Fig. 4(C). With the concentration of $NH_3 \cdot H_2O$ in MB increased to 0.4 mol/L, the particles of interior grape-stones-like cavities were obtained as shown in Fig. 4B. Up to 0.6 mol/L, the bigger particles with ca. 50 nm in diameter were obtained, and their porous interiors are clearly identified with ca. 3 nm in diameter as shown in Fig. 4(D). Obviously, ammonia concentration in MB plays an important role in tailoring interior structure of nanospheres. Insufficient amount of ammonia in MB

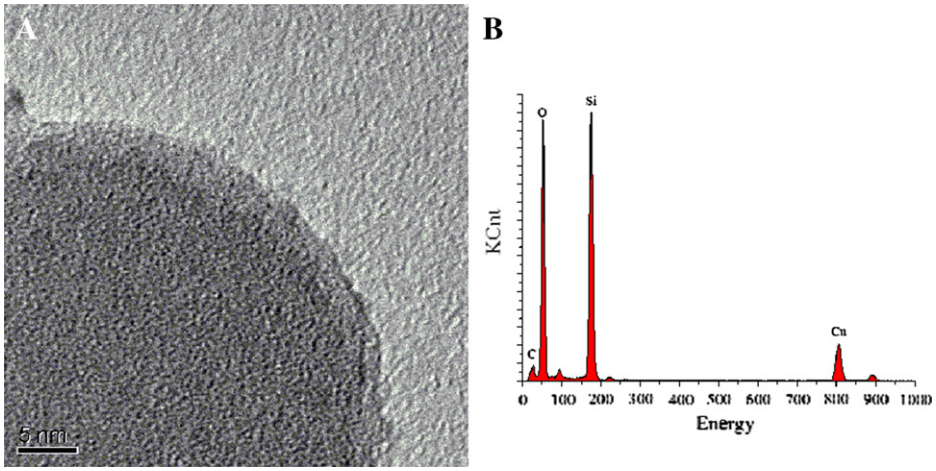

Fig. 3. HRTEM image (A) and EDX spectrum (B) of SiO_2 nanospheres shell.

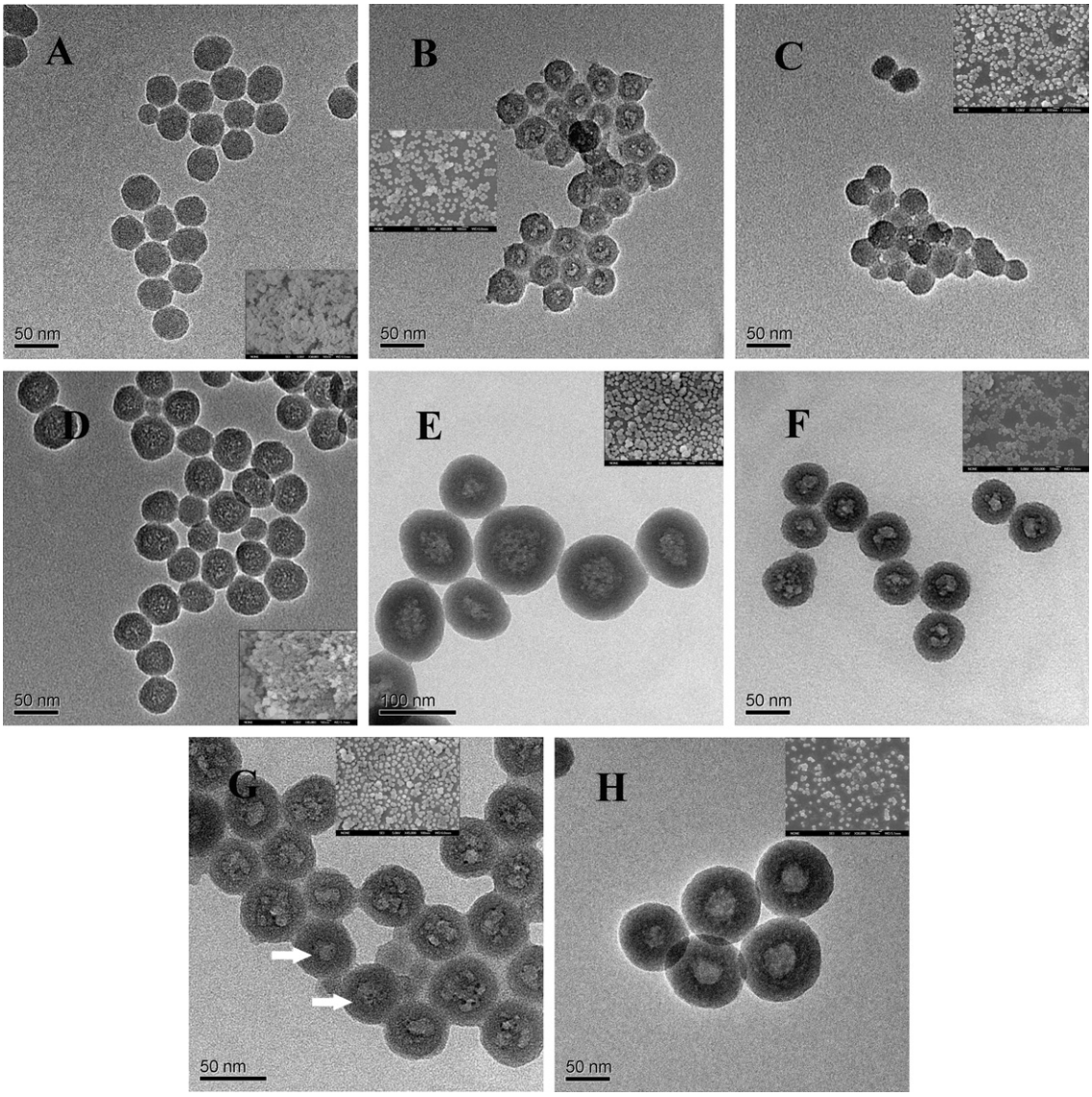

Fig. 4. TEM and SEM (inset) images of Sample 1 (A), Sample 2 (B), Sample 3 (C), Sample 4 (D), Sample 5 (E), Sample 6 (F), Sample 7 (G), Sample 8 (H).

cannot furnish enough OH^- for the precipitation of Zn^{2+}, so there are no templates in microemulsion droplets. The hydrolysis products of TEOS pass through the oil–water interface and aggregate to a certain extent to form dense spheres in the center of microemulsion droplets, as shown in Fig. 4(C). Moderate amount of ammonia in MB supplies enough OH^- to form zinc species in the microemulsion droplets, which aggregate as the temporary templates and etched gradually by MC, and the interior structure of grape-stone-like appears as shown in Fig. 4(B). While excessive ammonia in MB accelerates the precipitation of Zn^{2+}, thus more and smaller zinc species particles form [33,34], after the adding of MC and TEOS, the particles with much more porous interior are collected as shown in Fig. 4(D). The analysis above is further confirmed by the result of Fig. 4(E), in which twofold Zn^{2+} in MA and ammonia in MB was added. The bigger silica nanospheres with ca.100 in diameter and more closed-pack interiors with ca. 50 nm in diameter are identified in contrast with the result in Fig. 4(B). Furthermore, another critical factor aging time of temporary templates was investigated. As the time was extended from 0.5 to 12 h, the size of silica nanospheres in Fig. 4(F) became bigger with ca. 60 nm in diameter concomitantly with bigger grape-stone-like interior with ca. 30 nm in diameter than that in Fig. 4(B). As the time continued to be extended to 24 h, the morphologies of silica nanospheres changed very little, but the porous interiors became bigger or even formed single hollow interior (as indicated by white arrows) as shown in Fig. 4(G). While the time was extended to 48 h, hollow nanospheres with ca. 25 nm in shell thickness and ca. 40 nm in interior diameter were obtained as shown in Fig 4(H). It is concluded that with the aging time being prolonged, the in-situ zinc species nanocrystals aggregate and grow into larger or even single ones through Ostwald Ripening process, which act as temporary templates to form the grape-stone-like or single hollow interior nanostructures.

3.4. Formation mechanism of SiO_2 nanospheres with tailorable interior

Based on all the facts above, the possible formation mechanism of nanostructured interior of silica nanospheres is proposed and illustrated in Fig. 5. The primitive zinc species nanocrystals (b) functioned as the temporary templates are produced

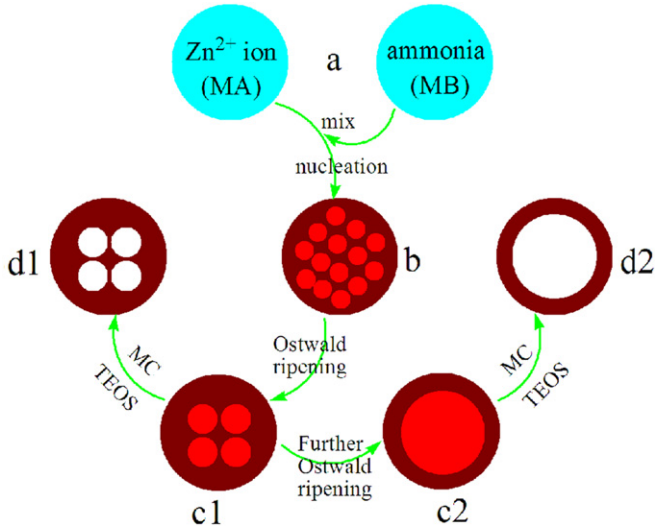

Fig. 5. Formation process of SiO_2 nanospheres with porous and single hollow interior.

immediately by the mixture of MA and MB (a) and tend to aggregate and grow. After the addition of MC containing concentrated ammonia, the aqueous droplets in MC are benefitted for the hydrolysis of TEOS and meanwhile etch the templates into the soluble zinc complex $Zn(NH_3)_4^{2+}$. There exists a reaction rate competition between hydrolysis of TEOS and etching of templates. To a certain extent, the surfactants prevent diffusion of concentrated ammonia into aqueous droplets of MA and MB from MC. In this case, the hydrolysis rate is slightly quicker than the etching rate and the nanostructured interior structure forms. As the growing time of primitive nanocrystals is shorter than 48 h, the nanocrystals scatter in the aqueous droplets and have not ripened into a single one (c1). Hydrolysis products of TEOS precipitate and aggregate around the templates, meanwhile the templates will be etched gradually by concentrated ammonia. SiO_2 nanospheres with porous interior are obtained due to the competitive reactions (d1). As the growing time is extended to 48 h, the primitive nanocrystals ripen into a larger single one (c2), then SiO_2 nanospheres with single hollow interior are obtained (d2). During the process, the primitive nanocrystals act as the growing seeds, which provide with the growth sites. They first serve as the templates shaping the interior structures of the nanospheres. With the progress of the reaction they are consumed, the porous interior structure will be obtained. Herein the aging time of temporary templates produced by MA and MB is decisive for either multiple interiors or single interior type. In other words, Ostwald ripening process is pivotal for achieving tailorable interior inside SiO_2 nanospheres. However, the intermediate core–shell structures were not discovered in this study. The possible reason is that the hydrolysis rate of TEOS and the etching rate of zinc species are very fast in the presence of concentrated ammonia, the details of which needs further study.

4. Conclusion

In this study, uniform nano-sized SiO_2 nanospheres with porous interior or single hollow interior were synthesized by means of a microemulsion technique. Nanostructured interior of SiO_2 particles could be tailored by controlling Zn^{2+} (in MA) and $NH_3 \cdot H_2O$ (in MB) species and the aging time of zinc species. Zn^{2+} and $NH_3 \cdot H_2O$ are able to produce precipitation $Zn(OH)_2$/ZnO as well as soluble zinc complex $Zn(NH_3)_4^{2+}$. Such characteristic of the two reactants has been successfully applied in this study. As the hydrolysis rate of TEOS is slightly quicker than the etching rate of templates, the SiO_2 shells form at the same time even in advance of the complete dissolving of the templates, and the nanostructured interior forms. And just controlling of aging time of temporary templates produced by MA and MB can construct porous or single hollow interior. Compared with other techniques, no additional processes such as roasting or dissolving are needed. This facile method is expected to be available in synthesizing porous or single hollow interior of other inorganic oxides.

Acknowledgment

This research is financially supported by the Knowledge Innovation Program of the Chinese Academy of Sciences (Grant no. KJCX1. YW. 07).

References

[1] F. Iskandar, A.B.D. Nandiyanto, K.M. Yun, C.J. Hogan, K. Okuyama, P. Biswas, Adv. Mater. 19 (2007) 1408–1412.
[2] S. Ikeda, S. Ishino, T. Harada, N. Okamoto, T. Sakata, H. Mori, S. Kuwabata, T. Torimoto, M. Matsumura, Angew. Chem. Int. Ed. 45 (2006) 7063–7066.
[3] H.G. Zhang, Q.S. Zhu, Y. Zhang, Y. Wang, L. Zhao, B. Yu, Adv. Funct. Mater. 17 (2007) 2766–2771.
[4] W.M. Zhang, J.S. Hu, Y.G. Guo, S.F. Zheng, L.S. Zhong, W.G. Song, L.J. Wan, Adv. Mater. 20 (2008) 1160–1165.
[5] X.W. Lou, L.A. Archer, Adv. Mater. 20 (2008) 1853–1858.
[6] O. Kreft, M. Prevot, H. Mohwald, G.B. Sukhorukov, Angew. Chem. Int. Ed. 46 (2007) 5605–5608.
[7] O. Kreft, A.G. Skirtach, G.B. Sukhorukov, H. Mohwald, Adv. Mater. 19 (2007) 3142–3145.
[8] W.R. Zhao, H.R. Chen, Y.S. Li, L. Li, M.D. Lang, J.L. Shi, Adv. Funct. Mater. 18 (2008) 2780–2788.
[9] J.H. Gao, G.L. Liang, J.S. Cheung, Y. Pan, Y. Kuang, F. Zhao, B. Zhang, X.X. Zhang, E.X. Wu, B. Xu, J. Am. Chem. Soc. 130 (2008) 11828–11833.
[10] X.W. Lou, C.L. Yuan, L.A. Archer, Small 3 (2007) 261–265.
[11] F.J. Suarez, M. Sevilla, S. Alvarez, T. Valdes-Solis, A.B. Fuertes, Chem. Mater. 19 (2007) 3096–3098.
[12] X.F. Wu, Y.J. Tian, Y.B. Cui, L.Q. Wei, Q. Wang, Y.F. Chen, J. Phys. Chem. C 111 (2007) 9704–9708.
[13] C.Z. Wu, Y. Xie, L.Y. Lei, S.Q. Hu, C.Z. OuYang, Adv. Mater. 18 (2006) 1727–1732.
[14] X.W. Lou, Y. Wang, C.L. Yuan, J.Y. Lee, L.A. Archer, Adv. Mater. 18 (2006) 2325–2329.
[15] P. Tartaj, T. Gonzalez-Carreno, C. Serna, J. Adv. Mater. 13 (2001) 1620–1624.
[16] Y.G. Sun, Y.N. Xia, Science 298 (2002) 2176–2179.
[17] Y.D. Yin, R.M. Rioux, C.K. Erdonmez, S. Hughes, G.A. Somorjai, A.P. Alivisatos, Science 304 (2004) 711–714.
[18] A. Cabot, V.F. Puntes, E. Shevchenko, Y. Yin, L. Balcells, M.A. Marcus, S.M. Hughes, A.P. Alivisatos, J. Am. Chem. Soc. 129 (2007) 10358–10360.
[19] S. Peng, S.H. Sun, Angew. Chem. Int. Ed. 46 (2007) 4155–4158.
[20] J.Y. Chen, B. Wiley, J. McLellan, Y.J. Xiong, Z.Y. Li, Y.N. Xia, Nano. Lett. 5 (2005) 2058–2062.
[21] H.P. Liang, L.J. Wan, C.L. Bai, L. Jiang, J. Phys. Chem. B 109 (2005) 7795–7800.
[22] F. Caruso, R.A. Caruso, H. Mohwald, Science 282 (1998) 1111–1114.
[23] J.R. Song, L.X. Wen, J.F. Chen, H.M. Ding, Aicam 11-12 (2006) 551–554.
[24] X.M. Guo, X.G. Liu, B.S. Xu, T. Dou, Colloids Surf. A: Physicochem. Eng. Aspects 345 (2009) 141–146.
[25] G.X. Liu, G.Y. Hong, J. Solid State Chem. 178 (2005) 1647–1651.
[26] J.X. Huang, Y. Xie, B. Li, Y. Liu, Y.T. Qian, S.Y. Zhang, Adv. Mater. 12 (2000) 808–811.
[27] S.F. Wang, F. Gu, M.K. Lu, Langmuir 22 (2006) 398–401.
[28] X.L. Yu, C.B. Cao, H.S. Zhu, Q.S. Li, C.L. Liu, Q.H. Gong, Adv. Funct. Mater. 17 (2007) 1397–1401.
[29] J.H. Schulman, W. Stoeckenius, L.M. Prince, J. Phys. Chem. 63 (1959) 1677–1680.
[30] K. Nakmoto, Infrared and Raman spectra of inorganic and coordination compounds,, Chem. Ind. Press, Beijing, 1986, pp. 231–235.
[31] T.W. Zerda, M. Bradley, J. Jonas, J. Mater. Lett. 3 (1985) 124–126.
[32] I. Artaki, M. Bradley, T.W. Zerda, J. Jonas, J. Phys. Chem-Us. 89 (1985) 4399–4404.
[33] J.J. Richardson, F.F. Lange, Crystal Growth Design 9 (2009) 2570–2575.
[34] G.H. Bogush, C.F. Zukoski, J. Colloid. Interf. Sci 142 (1991) 1–18.